Electrochemical methods for the determination of urea: Current trends and future perspective

Lorenzo Quadrini [a], Serena Laschi [a], Claudio Ciccone [b], Filippo Catelani [b], Ilaria Palchetti [a,*]

[a] *Department of Chemistry "Ugo Schiff", University of Florence, Via della Lastruccia 3-13, 50019, Sesto Fiorentino, FI, Italy*
[b] *Chemitec S.r.l., Via Isaac Newton 28, 50018, Scandicci, FI, Italy*

ABSTRACT

Urea is the final product of nitrogen metabolism in mammals. In human beings, it is a main indicator of liver and kidney activity and a marker for hemodialysis treatments. Furthermore, urea is used in many industrial processes, in agriculture and in the farm industries. Thus, it is important to evaluate the level of this compound in biological fluids, in environmental matrices and in food samples. Electrochemical sensors represent an interesting tool for simple, rapid, in-situ, in-flow monitoring of urea. This review focuses on the recent advancements in electrochemical sensors and biosensors for urea determination. An overview of the existing electroanalytical approaches for urea determination is presented, and some new strategies are discussed, particularly those based on nanostructuration of the electrode surface. Finally, a brief description of the role that Artificial Intelligence could have in overcoming selectivity issues and speed of the analysis is also discussed.

1. Introduction

Urea, also known as carbamide, is an organic compound with the chemical formula $CO(NH_2)_2$. In human beings, urea is a product of protein catabolism and helps in preventing acidosis or ionic decompensation caused by NH_4^+ [1]. Under normal conditions, the bloodstream concentration of urea varies from 15 to 40 mg/dl (2.5–7.5 mM) [2]. Monitoring the amount of urea has always been of primary interest to the whole clinical diagnostic, since urea is a main indicator of liver and kidney activity and a marker for hemodialysis treatments. Some examples of commercial point-of-care analyzers of urea in clinical settings are reported in Table 1. Whereas, in Table 2 are reported the concentration range of urea in some biological fluids.

Apart its physiological role in mammals, urea is a compound with significant industrial applications. It is used in agriculture in combination with other nitrogenous fertilizers to increase the productive capacity of a soil [17–19]. Urea is also used as a component in skin care products [20], in cleaning products, in certain medicines, in urea–formaldehyde plastics or as a supplement in the diet of animals on intensive livestock farms [21]. The market demands for urea is expected to grow at 2% per annum, reaching 211.5 million metric tons by 2026 [22]. The main sources of urea in the environment are municipal, industrial, and agricultural waste and sewage systems, including the waste

from intensive livestock farms [23]. The fact that urea ends up in water reservoirs and watercourses creates eutrophication problems [24] and it is correlated with the outbreaks of several harmful algal blooms in several estuarine environments [25]. There is a general consensus to fix the maximum acceptable concentration of urea in wastewater at 12 mM in wastewater [26], but this value drops to 0.16 mM in water for human consumption [27].

Thus, even though the analytical methods reported in literature for the determination of urea have largely focused on clinical applications, there is a growing demand for reliable, robust, instrumentation and methodologies for the determination of urea in food and environmental samples. Indeed, a wide variety of analytical techniques have been developed for urea determination, including spectrophotometric, chromatographic, and electrochemical methods, with no single technique dominant in all areas, because of the diversity of applications [28]. These methods can be briefly classified as indirect methods or direct methods. Enzymatic hydrolysis with urease (EC 3.5.1.5) is generally performed and then ammonia and carbon dioxide can be optically [29] or electrochemically [30] measured to stoichiometrically determine indirectly the urea concentration. Direct methods for urea determination are instead commonly based on urea complexation with a ketone or an aldehyde (such as xanthydrol or diacetyl monoxime), under strong acidic conditions to form a product which is then measured either colorimetrically or by using an HPLC-based method [31,32]. The use of

* Corresponding author.
E-mail addresses: lorenzo.quadrini@unifi.it (L. Quadrini), ilaria.palchetti@unifi.it (I. Palchetti).

Abbreviations

AI =	Artificial Intelligence
BSA =	Bovine Serum Albumin
CMFC =	Ceramic-Based Microbial Fuel Cell
CNT =	Carbon Nanotubes
CPE =	Carbon Paste Electrode
CV =	Cyclic Voltammetry
DPV =	Differential Pulse Voltammetry
EDC =	1-Ethyl-3-[3-Dimethylaminopropyl]Carbodiimide hydrochloride
EDTO =	3,4-EthyleneDioxyThiOphene
EIS =	Electrochemical impedance spectroscopy
EO =	Equilibrium Optimizer
Fc-PAMAM =	Ferrocene-Poly(amidoamine)
FET =	Field Effect Transistor
FTO =	Fluorinated-Tin Oxide
GNDs =	Graphitized Nanodiamonds
GNPlts =	Graphene nanoplatelet
GO =	Graphene Oxide
HPLC =	High-performance liquid chromatography
ISE =	Ion-Selective Electrodes
ITO =	Indium Tin Oxide
LDH =	Layered Double Hydroxide
LOD =	Limit of Detection
LOQ =	Limit of Quantitation
ML =	Machine Learning
MCPE =	Modified Carbon Paste Electrode
MGCE =	Modified Glassy Carbon Electrode
MIP =	Molecular Imprinted Polymers
MWCNT =	Multi-Walled Carbon Nanotubes
NC =	NitroCellulose
Nf =	Nafion
NFMAS =	NanoFiber-Based Microfluidic Analysis System
NHS =	N-hydroxysulfosuccinimide
Ni-MOF =	Nickel-Metal–Organic Framework
NiS =	Nickel Sulfide
NPs =	NanoParticles
P(3HT-co-3TAA) =	Poly(3-HexylThiophene-co-3-ThiopheneAcetic Acid)
PANI =	Polyaniline
PEDOT	PSS = Poly(3,4-EthyleneDioxythiophene) PolyStyrene Sulfonate
PET =	Polyethylene Terephthalate
PMMA =	Poly(Methyl MethAcrylate)
PPy =	PolyPirrole
PS =	Polystyrene
PUFC =	Photocatalytic Urea Fuel Cell
PVA =	Polyvinyl Alcohol
PVC =	PolyVinyl Chloride
PVdF-HFP =	PolyVinylidene Fluoride-co-HexaFluoroPropylene
RE =	Reference Electrode
SF =	Silk Fibroin
SPE =	Screen Printed Electrode
SSE\Nianodized =	Ni nanotube-modified Stainless-Steel Electrodes
SSE\Zn =	Zn nanowire Stainless-Steel Electrodes
UOR =	Urea Oxidation Reaction
Urs =	Urease
μTED =	Thread-based Microfluidic Electroanalytical Device

Table 1
Examples of commercial devices for urea quantification in clinical settings.

Supplier	Commercial name	Transduction	Reference
ESAMED	SDI	Optical	[3]
Lifetest Vet Equipment ApS	InSight Minichem Analyzer	Optical	[4]
Hangzhou Lysun Biotechnology Co., Ltd	Lysun	Optical	[5]
Abbott Point Of Care Inc.	i-Stat	Electrochemical	[6,7]
Siemens Healthineers	epoc® Blood Analysis System	Electrochemical	[8]
Edan Instruments	EDAN i15	Optical	[9]
Radiometer Medical ApS	ABL90 FLEX PLUS blood gas analyzer	Electrochemical	[10,11]

Table 2
Average concentration ranges of urea in biological fluids.

Matrix	Urea Range (mM)	Reference
Blood	2.5–7.5	[12]
Urine	1.2–3.3	[13]
Saliva	1.2–7.8	[14]
Sweat	0–50	[15]
Milk	3.0–6.6	[12,16]

electrochemical sensor and biosensor technology for urea measurement is an interesting approach which possesses technical simplicity, low cost, and suitability for in-field analysis. Electrochemical sensors and biosensors can be taken to the sampling sites, having results in real time [33–35]. The first electrochemical urea biosensor was reported by Guilbault and Montalvo [36]. In that approach a glass electrode was used to detect ammonium ion activity by urease-catalyzed hydrolysis [37–41]. Over the time, neutral carrier-type ion-selective ammonium (NH_4^+) electrodes [42,43], gas-permeable ammonia [44] or carbon dioxide (CO_2) [40] electrodes, replaced the first employed glass electrode. Nowadays, different electrical and electrochemical transducers have been reported including Field Effect Transistor (FET) [45], potentiometric all solid-state electrodes, and amperometric transducers [46]. Also in this case, both direct and indirect electrochemical methods can be carried out. In the case of direct electrochemical measurements, a quantification of urea can be performed by measuring the current density resulting from its direct oxidation reaction [47–50], whereas in the case of indirect quantification electrochemical measurements can be carried out by monitoring the urea hydrolysis reaction. A plethora of novel electrode materials has been proposed for both direct and indirect electrochemical urea measurements [30].

Several reviews have been published recently on electrochemical sensors and biosensors technology for the detection of urea, but these are mainly focused on clinical applications [51] and on potentiometric transducers [12,30]. Thus, the aim of this review is to provide an updated revision of the literature in the last 5 years showing the current trends and future perspective (beyond the solely potentiometric and enzymatic biosensors) in terms of electrochemical transducer materials and sensor formats for urea electrochemical (bio)sensors assembly. Different examples of direct and indirect electrochemical methods for urea determination are here described. Moreover, the role of AI in improving the analytical performance of the sensors and in the optimization of working parameters is also discussed.

2. Direct electrochemical method for urea determination

Direct electrochemical measurement means that the analytical signal can be directly correlated with the concentration of urea in the sample.
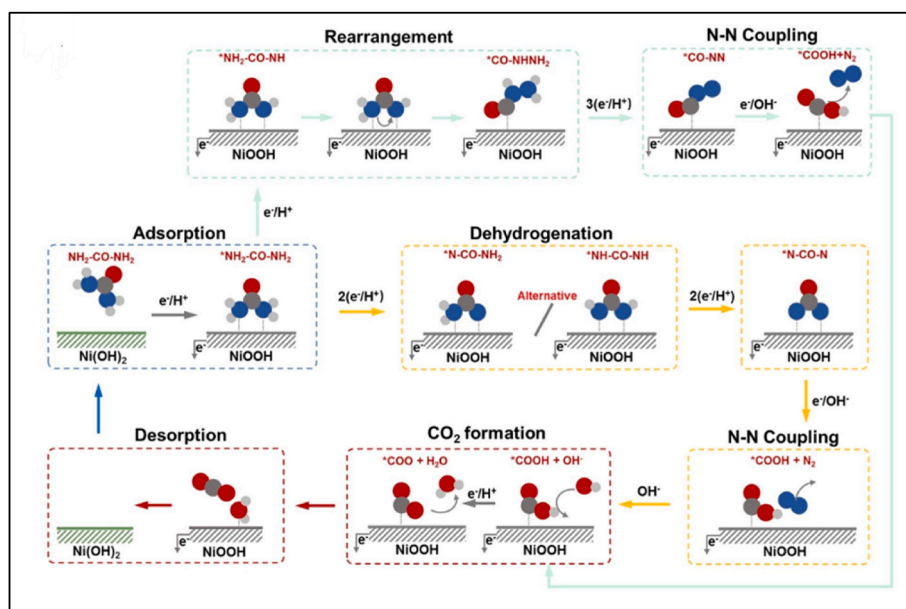
Fig. 1. Scheme of a proposed electrochemical urea oxidation under alkali conditions. (Reproduced with permission from Ref. [54]).

Table 3
Some examples of direct urea electrochemical sensors and their analytical performances.

Materials	Electroanalytical method	Linearity Range (M)	Detection Limit (M)	Real Sample	Reference
Polyvinylidene Fluoride-co-Hexafluoropropylene (PVdF-HFP)/Ni-Co nanofiber/	Amperometric	$2 \times 10^{-5} - 2.0 \times 10^{-3}$	1.2×10^{-5}	Urine	[55]
NiCo$_2$O$_4$ NNs/GCE	CV	$1 \times 10^{-5} - 5 \times 10^{-3}$	1.0×10^{-6}	Urine	[56]
Nafion/ (Ni-MOF)NBs/GCE	LSV	$1 \times 10^{-5} - 7.0 \times 10^{-3}$	2.23×10^{-6}	Urine	[57]
NiOOH/Ag/Carbon paper	Amperometric	$2 \times 10^{-4} - 26.0 \times 10^{-3}$	5.0×10^{-6}	Urine	[58]
Ni NTs/Stainless Steel Electrode	Amperometric	$3 \times 10^{-6} - 2 \times 10^{-2}$	3×10^{-6}	Tap Water	[59]
NiS/Graphene Oxide/GCE	DPV, Impedimetric	$1 \times 10^{-4} - 1.0 \times 10^{-3}$	3.79×10^{-6}	Milk	[60]
NiS/GO/CPE	Amperometric	$1 \times 10^{-4} - 6.0 \times 10^{-3}$	7.02×10^{-6}	Saliva	[14]
LaNi$_{0.6}$Fe$_{0.4}$O$_3$-CeO$_2$ (LNF-C)/MWCNT/ITO	Amperometric	$25 \times 10^{-6} - 670 \times 10^{-6}$	1×10^{-6}	Urine	[61]
Ni-metal organic framework/MWCNT/ITO	Amperometric	$1 \times 10^{-5} - 1.12 \times 10^{-3}$	3×10^{-6}	Urine	[62]
Graphene-PANI	Amperometric	$10 \times 10^{-6} - 200 \times 10^{-6}$	5.88×10^{-6}	Tap Water Milk	[63]

NNs: nanoneedles; NBs: nanobelts; NTs: nanotubes; MWCNT: Multi-Walled Carbon Nanotubes; ITO: Indium Tin Oxide; CNT: Carbon Nanotubes; PPY: PolyPirrole; PANI: Polyaniline; SPE: Screen Printed Electrode; CV: Cyclic Voltammetry; DPV: Differential Pulse Voltammetry.

These methods are mainly based on amperometry or voltammetry and are related to the urea redox reaction at the electrode surface. The redox reaction is driven by an applied potential and led to a current density value proportional to the concentration of urea in the bulk of the solution. This type of measurement is generally performed by using selected electrode materials or by modifying traditional electrode surfaces with innovative nanomaterials. Indeed, the nanostructuration of the electrode surface, increases the surface area of the electrode, improving the analytical signal [52]. In recent years, it has been shown that Ni is an excellent catalyst for urea oxidation reaction (UOR), with a low cost compared to Pt and Pd [53]. The catalytic oxidation process promoted by nickel-based materials has been studied with a particular focus on alkali conditions [47–50] (Fig. 1). The surface area of the nickel electrode is firstly chemically oxidized to Ni(OH)$_2$ by the alkaline solution; then the Ni(OH)$_2$ undergoes oxidation to its active NiOOH form due to the high potential value applied at the electrode during the urea adsorption step, as shown in Fig. 1; then, the NiOOH oxidizes urea to regenerate Ni(OH)$_2$; the total balance of the reaction is (1):

$$CO(NH_2)_2 + 6OH^- \rightarrow N_2 + 5H_2O + CO_2 + 6e^- \quad (1)$$
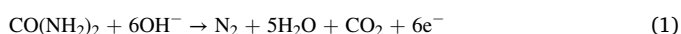
Hence, NiOOH acts as the catalytic active form. However, the current

density is generally low because of the unavailability of NiOOH active sites. To overcome these problems, attempts have been made to develop different kind of nanomaterials, because, as it is well known, the surface area of nanomaterials are larger than those of macro counterparts. This property contributes to the increase of the number of active sites, and thus to a more efficient catalytic behavior.

In addition to enhancing the catalytic activity and specific surface area, it's worth noting that expediting the desorption of CO from the electrode surface is crucial since it is the slow step of the reaction. Therefore, there is the interest in developing alternative nanomaterials or nanocomposites for accelerating this process.

Different examples of Ni nanocomposites, i.e. nanofibers [55], nanoneedles [56] nanobelts [57], nanorods [58] nanotubes [59] have been reported in literature as shown in Table 3 and in Fig. 2.

A nanostructured Ni-based sensor for urea monitoring in milk sample was reported in Ref. [60]. In this case a graphene stabilized nickel sulfide electrode was used. Nickel Sulfide/Graphene Oxide (NiS/GO) nanocomposites were obtained by a superficial hydrothermal process on a modified Glassy Carbon Electrode (NiS/GO/GCE). A LOD and LOQ of 3.79 and 12.6 μM, respectively, were found. Moreover, NiS/GO/GCE demonstrated robustness for the detection in real sample with a recovery
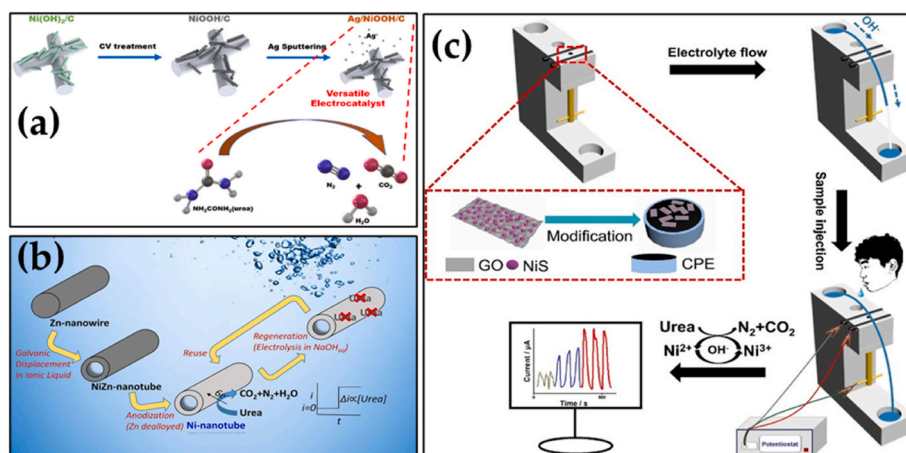
Fig. 2. Different examples of Ni-nanocomposites for urea detection. (a) Silver (Ag)/NiOOH nanorods prepared by a cyclic voltammetry treatment of the Ni(OH)$_2$ precursor and sputter deposition of Ag (Reprinted with permission from Ref. [58]. Copyright 2020 American Chemical Society.); (b) Overall process of modification of a stainless-steel electrode modified with ZnNi-Nanotubes and urea measurement (Reproduced with permission from Ref. [59]); (c) Schematic illustration of thread-based microfluidic electroanalytical device (μTED) for detecting urea. The μTED consists of a carbon paste electrode (CPE) modified by NiS/Graphene Oxide (GO) and cotton threads as microfluidic channels (Reproduced with permission from Ref. [14]).
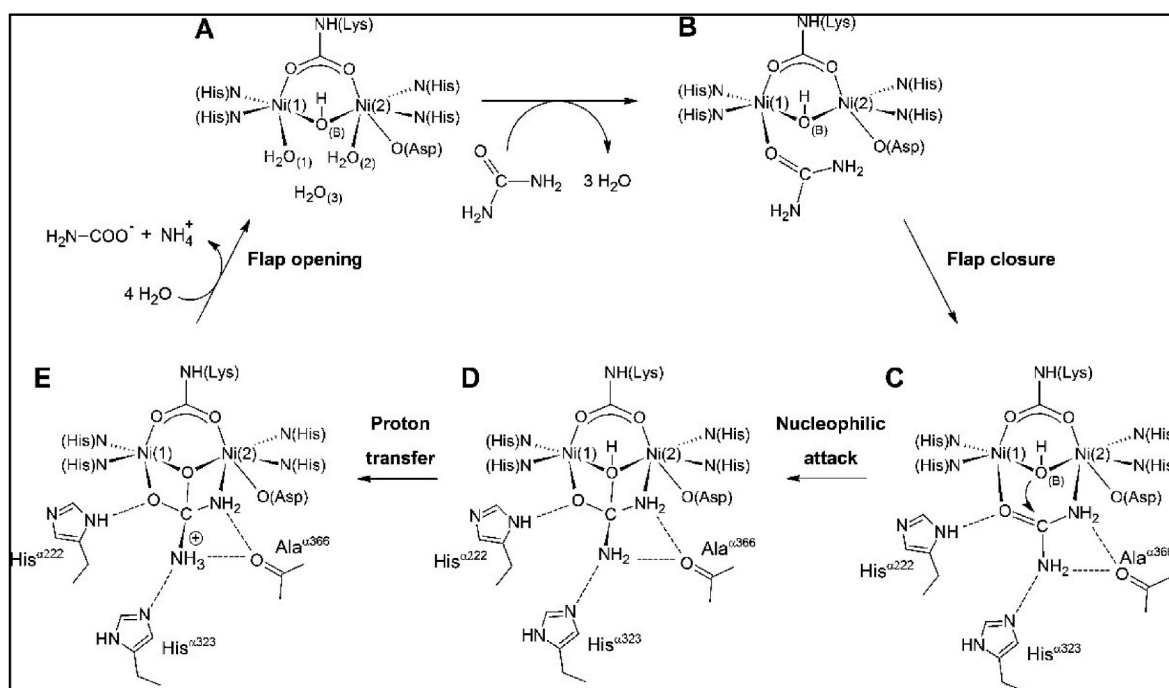

Fig. 3. Scheme of the catalytic mechanism of urease. The neutral imidazole side chain of the active site conserved histidine residue, moving nearer the active site upon closure of the flap, stabilizes the nascent C–NH$_3^+$ group (5E). The distal C–N bond is broken, ammonia is released, and the resulting carbamate decomposes into NH$_4^+$ and bicarbonate. The flap opening could facilitate the release of products and allow bulk water to rehydrate the active site to yield the native state of the enzyme (5A). These steps could occur in a concerted manner. This mechanism agrees with all kinetics data, in particular the pH-dependence of the enzyme activity and the noncompetitive inhibition by fluoride, thought to replace the bridging hydroxide.. (Reprinted with permission from Ref. [67]. Copyright 2011 American Chemical Society.).

percentage of 98.6–99.4%.

Recently, a NiCu(OOH)/Polystyrene (PS) electrode was used for the development of a wearable biosensor [64]. PS provided a porous structure, leading to an enough number of active sites, easy access to reactants, and adequate water wettability for effective charge transfer. The modified surface was obtained through co-sputtering of Ni-Cu alloy as catalyst.

A microfluidic electroanalytical device, allowing the quantification of urea in saliva is reported in Ref. [14]. A Cotton thread pad was used as microfluidic sampling channel and a NiS/GO/Carbon Paste Electrode

(CPE) was developed as urea-sensitive sensor. Two graphite rods (Ø = 3.0 mm) were used as auxiliary electrode and pseudo-reference electrode, respectively, together with NiS/GO/CPE as working electrode. The system is shown in Fig. 2c. This amperometric sensor allowed to detect urea in the concentration range from 0.1 mM to 6.0 mM.

As reported in literature, direct amperometric measurement of urea is an interesting approach, as there is no need for an enzymatic component that may undergo a change in activity with time (stability issue) or may increase the cost of the measurements. By contrast the selectivity, in absence of the biocatalyst, could be compromised. The
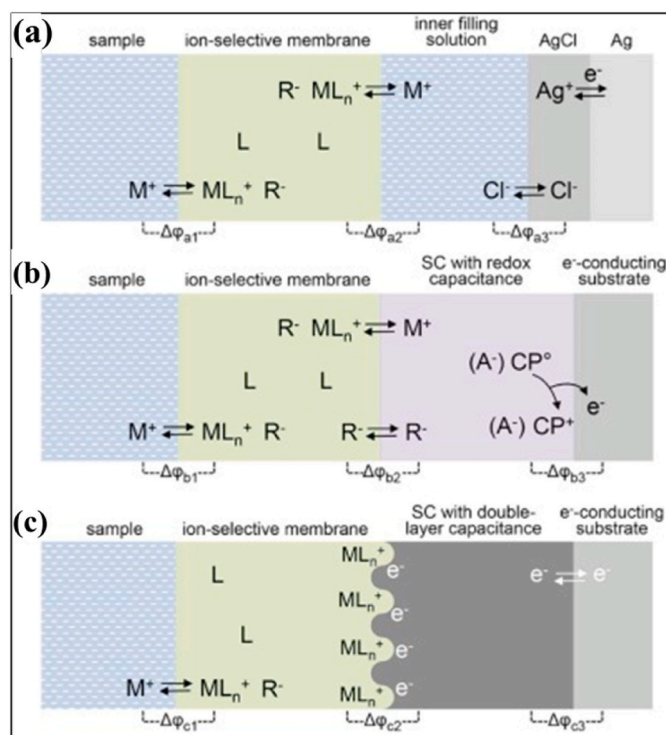
Fig. 4. Schematic representation of all relevant interfaces within different types of ISEs with cation (M^+) selective membranes that contain an electrically neutral ionophore (L) and anionic sites (R^-): (a) a conventional ISE with an inner filling solution; (b) an all-solid-state ISE based on an anion (A^-, R^-) doped-conducting polymer (CP) solid contact (SC) with a high redox capacitance; (c) an all-solid-state ISE based on a high-surface-area SC exhibiting a high double layer capacitance. (Reproduced with permission from Ref. [74]).

interference from other electroactive species could also be a major issue, leading to inaccurate results. From this point of view chemometric methods, machine learning (ML), and Artificial Intelligence (AI) could help in overcoming selectivity issues [65,66]. Critically analyzing the literature, it has to be highlighted that the analytical performances of the reported systems are basically compatible with clinical (see Table 2) or environmental requirements. By contrast, in some cases, it not well explained the complexity of the surface modification and the role of the different nanocomposites and their morphologies in achieving the required analytical performance.

3. Indirect electrochemical methods based on catalytic biosensors for urea determination

Indirect urea determination can be performed by using both potentiometric and amperometric biosensors.

The most common bioreceptor for urea determination is the enzyme urease, a nickel-containing metalloenzyme [67] that hydrolyzes urea into CO_2 and NH_4^+ ions, following the scheme reported in Fig. 3.

Many examples of potentiometric urease-based biosensors are reported in literature. Coupling a potentiometric measurement with the enzymatic catalysis means that high selectivity can be achieved due to the high affinity and selectivity that the enzyme possesses for the substrate and to the fact that potentiometric transducers, such as the ion-selective electrodes (ISEs) for NH_4^+, very selectively detect the products of the enzymatic hydrolysis reaction. Nevertheless, potentiometric urea biosensors face interference from competing species such as uric acid, Na^+ K^+ and Ca^{2+} ions, which results in high detection limits and slow response times [68]. Coupling urease-based catalysis with an amperometric measurement is also feasible and some examples are reported in literature. Furthermore, other bioreceptors have been recently

explored such as aptamers and Molecular Imprinted Polymers (MIPs) [69,70].

In the following sections, indirect urea determination is reviewed as enzymatic-based electrochemical biosensors and non-enzymatic electrochemical biosensors. Literature is revised considering the electroanalytical technique used (i.e., potentiometry vs amperometry).

3.1. Potentiometric enzyme-based biosensors

As already mentioned, urease catalyzes the conversion of urea to NH_3 and CO_2, which then dissociates to NH_4^+ and bicarbonate HCO_3^- ions in solution. Thus, urea measurement can be performed through NH_3, CO_2, NH_4^+, and pH variations.

The NH_4^+ ions are detected using various type of potentiometric transducers (Fig. 4), including conventional liquid-membrane, all solid-state and gas-permeable membrane ISEs [68,69]. Conventional liquid membrane ISEs use ionophores embedded in a hydrophobic membrane to selectively bind NH_4^+ ions, generating a potential variation proportional to the NH_4^+ activity [71,72]. Liquid-membrane ISEs contain liquid contacts (typically referred to as inner filling solutions) that separate the sensing membrane from the inner reference electrode [71]. All solid-state ISEs employ an electron-conducting layer, such as conductive polymers, metal oxides or porous carbon, that interacts with NH_4^+ ions, causing a change in electrical properties measured potentiometrically against a reference electrode [73]. In all solid-state ISEs, a solid contact is formed between the sensing membrane and an electron-conducting layer to replace the liquid contact, serving as an ion-to-electron transducer. Note that all-solid-state ISEs are not to be confused with ISEs that comprise a solid-state ion-selective membrane (such as the fluoride electrode based on LaF_3) [74].

Gas-permeable membrane ISEs convert NH_4^+ to NH_3 gas, which diffuses across a selective gas membrane and reacts with a sensing solution, altering the pH in a concentration-dependent manner. Then, the variation in pH is measured by a pH sensitive glass electrode [75]. CO_2 is commonly measured by a Severinghaus-type electrode, based on normal pH-glass electrode with a bicarbonate-electrolyte around the tip, separated from the sample by a gas-membrane permeable to CO_2. The pH of bicarbonate resets according to the local pCO_2 and can be measured with the pH-sensor. In all cases, for gas permeable ISEs a temperature-compensation is needed.

Potentiometric transducers offer simple, selective, inexpensive means of detecting the products of the urease reaction to determine urea concentrations and for this reason potentiometric urease-based biosensors have demonstrated to be a robust platform for urea detection. Some commercial instrumentations that take advantage of potentiometric urease-based biosensors are reported in Table 1 [76].

Many procedures have been developed over the years for the fabrication of urease-based biosensors. Nowadays, new approaches based on thick- and thin-film technologies are used to mass produce miniaturized, cost-effective, reproducible, calibration-free transducers [77] that fit quite well with the requirements of point-of care or point-of needed analyzer. A thick-film sensor comprises layers of special pastes (thickness 10–50 μm) deposited onto an insulating substrate; the method of film deposition is the screen-printing technique [78]. Thin-film electrochemical transducers are built up by the successive deposition and patterning of dielectric and conductive materials, on top of an optically flat and polished substrate. The deposition of the thin metallic films (thickness 10–200 nm) is generally carried out by classical evaporation or sputtering of a solid metal source; then, photolithography and other techniques can be envisaged to pattern the electrode material. Using these technologies, disposable microfabricated arrays of sensors and biosensors have been developed.

The potential usefulness of nano- and micro-structured materials and composites in potentiometric applications (both as transducers and receptor phases in ion-selective electrodes) continue to be deeply explored [79–106]. In one of these approaches as an example, urea detection was
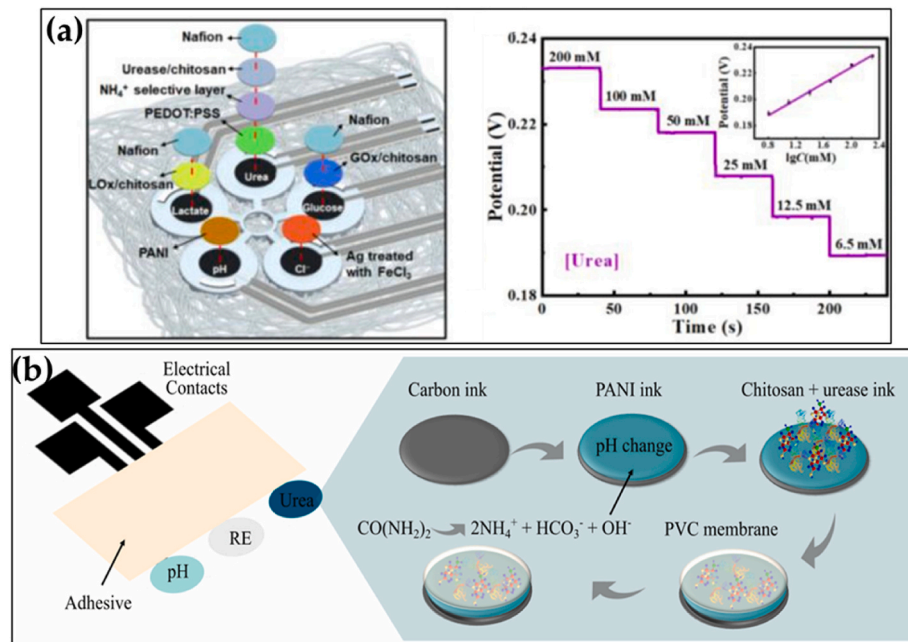
Fig. 5. (a) Schematic illustration of the multilayer assemblies in an exploded view, including glucose, lactate, Cl^-, urea and pH sensing units and Open Circuit Potential response for relevant levels of urea (Polyaniline (PANI), Graphene Oxide (GO), poly(3,4-ethylenedioxythiophene) polystyrene sulfonate (PEDOT:PSS)) (Reproduced with permission from Ref. [107]), (b) Representation of the potentiometric sensors for pH monitoring and detection of urea in sweat and schematic treatment of the electrode surface (PANI, Polyvinyl chloride (PVC), Reference Electrode (RE)) (Reproduced with permission from Ref. [108]).

Table 4
Some examples of indirect urease-based potentiometric sensors recently reported in literature with the kind of real samples analyzed and the reported analytical features.

Materials	Measure	Linearity Range (M)	Detection Limit (M)	Real Sample	Response Time (sec)	Stability (days)	Reference
Urs-Chitosan- encapsulated/PANI-grafted ZnO	Potentiometric	$3 \times 10^{-4} - 8 \times 10^{-3}$	5×10^{-4}	Blood	180	56	[79]
Urs-Poly(2-hydroxyethyl methacrylate-glycidyl methacrylate) nanoparticles	Potentiometric	$1 \times 10^{-5} - 5 \times 10^{-1}$	7.7×10^{-7}	Artificial Serum	30	90	[82]
Urs-COO-PVC(Nonactin)	Potentiometric	$10^{-4} - 10^{-2}$	1.0×10^{-4}	Urine	60 to 120	20	[85]
Recombinant Urs-PVA/Styrylpyridinium (SbQ) photopolymer	Potentiometric	$5 \times 10^{-4} - 1.5 \times 10^{-2}$	1×10^{-4}	Blood	60 to 120	150	[88]
Urs- γ-Al_2O_3	Potentiometric	$3.0 \times 10^{-5} - 1.4 \times 10^{-2}$	10×10^{-6}	Urine	120 to 240	90	[89]
Urs-PVA & polyacrylamide (PAA)	Potentiometric	$1 \times 10^{-3} - 1$	1×10^{-3}	Blood Serum	120	–	[90]
Urs-Imprinted TiO_2	Potentiometric	$8 \times 10^{-6} - 3 \times 10^{-3}$	5.0×10^{-6}	Urine	25	30	[91]
Urs-Fullerene-Poly(n-butyl acrylate)-Hydrogen Ionophore	Potentiometric	$4.2 \times 10^{-5} - 1.2 \times 10^{-3}$	–	Urine	<120	140	[93]
Urs-Nylon	Potentiometric	$1.6 \times 10^{-5} - 3.3 \times 10^{-4}$	–	Sugar Cane Vinasse	900	70	[94]
Urs-Poly(acrylonitrile–methylmethacrylate–sodium vinylsulfonate)	Potentiometric	$1 \times 10^{-3} - 1 \times 10^{-1}$	3×10^{-4}	Milk	120	70	[96]
Urs-Fe_3O_4 Paramagnetic Particles-Polyelectrolyte Microcapsules	Potentiometric	$3 \times 10^{-5} - 1 \times 10^{-1}$	3×10^{-5}	Milk	30 to 150	30	[97]
Urs-Chitosan	Potentiometric	$5 \times 10^{-4} - 10^{-2}$	1×10^{-4}	Serum	30 to 120	60	[98]
Urs-Polypyrrole/Carbon Paper	Potentiometric	$1.22 \times 10^{-6} - 3.85 \times 10^{-3}$	1×10^{-6}	Serum	60 to 100	>30	[99]
Urs-Tetraphenylborate doped Polyaniline	Potentiometric	–	20×10^{-6}	Serum Milk	–	60	[100]
Urs-Poly(carbamoylsulphonate) (PCS) + polyethyleneimine (PEI)	Potentiometric	–	2.5×10^{-5}	Milk	30 to 40	8	[104]
Nafion-Urease + Chitosan-PEDOT.PSS/NH_4^+ selective layer	Potentiometric	$6.4 \times 10^{-3} - 200 \times 10^{-3}$	1.3×10^{-3}	Sweat	900	28	[107]
PVC-Chitosan + Urease-PANI-Screen Printed Electrode	Potentiometric	$5 \times 10^{-3} - 200 \times 10^{-3}$	—	Sweat	150	<10	[108]

Urs: Urease; PVC: Polyvinyl Chloride, PANI: Polyaniline; PVA: Polyvinyl Alcohol; NC: Nitrocellulose; GO: Graphene Oxides; PET: Polyethylene Terephthalate, PVC: Polyvinyl Chloride, MWCNT: Multi-Walled Carbon Nanotubes; ITO: Indium Tin Oxide; BSA: Bovine Serum Albumin; EDC: 1-Ethyl-3-[3-dimethylaminopropyl]carbodiimide hydrochloride; NHS: N-hydroxysulfosuccinimide; CNT: Carbon Nanotube.
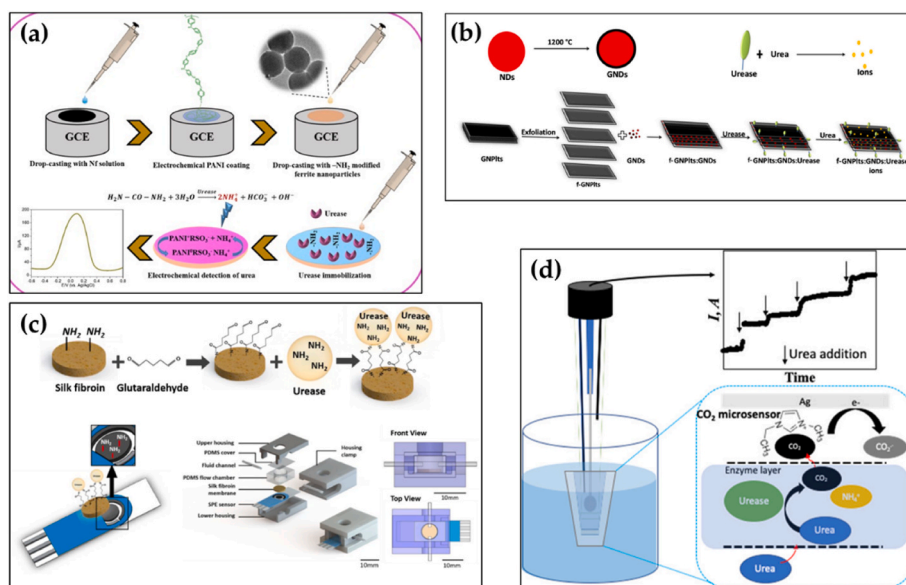
Fig. 6. (a) Procedure for Urease/CuF/PANI/Nf(GCE biosensor preparation and a schematic illustration of NH_4^+ detection mechanism (Reproduced with permission from Ref. [114]), (b) Schematic for the graphitization of nanodiamonds (NDs) by heating at 1200 °C in the presence of argon, hydrolysis of urea into ions by the urease, incorporation of graphitized nanodiamonds (GNDs) into layers of exfoliated f-GNPlts and the capture of ions onto the composite surface upon the hydrolysis of urea. (Reproduced with permission from Ref. [115]), (c) Schematic diagram of the principle of immobilization of urease on the silk fibroin (SF) membrane, the amination of the surface of the carbon electrode, and the configuration of the sensor system (Polydimethylsiloxane (PDMS), Screen-printed electrodes (SPEs)) (Reproduced with permission from Ref. [116]), (d) Schematic representation of the urea microsensor based on the CO_2 microsensor. The CO_2 produced from urea hydrolysis diffuses through the gas permeable membranes of the CO_2 microsensor and is detected through reduction at an Ag cathode. (Reproduced with permission from Ref. [117]).

facilitated by a four-layer structure containing a poly(3, 4-ethylenedioxythiophene) polystyrene sulfonate (PEDOT:PSS) conductive layer, a NH_4^+-selective layer, an enzymatic layer (urease/chitosan) and a Nafion (Nf) layer [107]. This flexible device can be conformally and harmlessly attached to the skin surface, and was used to the simultaneous quantification of glucose, lactate, pH, Cl^- and urea, Fig. 5a. The reported LOD for the urea was 1.3 mM with a sensitivity of 31.4 mV per decade of concentration.

Ibáñez-Redín et al. [108] developed a wearable potentiometric biosensor for urea sensing in sweat. The sensor is based on a screen-printed carbon electrode modified with polyaniline ink, urease bioink and a polyvinylchloride membrane (Fig. 5b). Urea detection was performed in a wide concentration range (from 5 to 200 mM), encompassing urea levels in human sweat. The biosensor had a 5 min response time and did not show interference from other substances in sweat. Some other examples of enzyme-based potentiometric biosensor are also shown in Table 4.

3.2. Amperometric and impedimetric enzyme-based biosensors

As for the potentiometric-based biosensors, recent advances in nanomaterials, conductive polymers, electrode modifications, and immobilization techniques have significantly improved the performance of amperometric urease-based biosensors, enhancing their sensitivity, selectivity, and stability. Among other nanomaterials, graphene [109, 110] and carbon-nanotubes [111] have been frequently used. Thus, in comparison to few decades ago, when potentiometric transducers were the solely used, nowadays different examples of amperometric biosensors are reported in literature, with analytical performances not far from the potentiometric counterpart.

Dervisevic et al. [112], developed a biosensor using ferrocene-poly (amidoamine) (Fc-PAMAM) dendrimers combined with MWCNTs and urease. In this approach the electrochemical signal is related to the electron transfer of ferrocene linked in the dendrimer. The polymer can change its spatial conformation depending on the pH that is locally

modified on the electrode surface during the urea hydrolysis process. The biosensor exhibits a linear range of 0.2–1.8 mM with a LOD of 0.05 mM. This biosensor was used to detect urea in human blood.

Iron-based nanoparticles were largely used to indirect urea quantification, due to their chemical stability, mechanical hardness and low toxicity. As an example, Fe_3O_4/MWCNT/PANI-Nafion (Nf) nanocomposites [113] or Fe_3O_4/Cu/PANI-Nf [114] were coupled to urease for the modification of GCEs (Fig. 6a). In these two approaches the biocatalytic process of urea hydrolysis generates NH_4^+ ions on the surface. The NH_4^+ ions bind to PANI. The electroactive species then is the PANI-NH_4^+ that gives an amperometric signal that could be correlated to the concentration of urea in the solution. In the case of Fe_3O_4/Cu/PANI-Nf/urease nanocomposite a LOD of 0.17 μM and a wide linear range of 0.5–45.0 μM were obtained.

Kumar and his group [115] (Fig. 6b) developed a graphene nanoplatelet (GNPlts)/Graphitized Nanodiamonds (GNDs)/Urease using a self-organization process. The ions generated by the addition of urea, thanks to the urease immobilized on the surface of the nanocomposite, alter the electron transport parameters (e.g., the mobility of electrons, conductivity, and Dirac point shifting). Changes in these parameters led to the appearance of a current.

Urease, immobilized onto Silk Fibroin (SF) scaffolds mounted in a polydimethylsiloxane (PDMS) sensor housing, as shown in Fig. 6c, was proposed by Kim et al. [116] for urea measurement in flow conditions. This urea biosensor elicited a linear current-concentration response in a range from 0.1 to 20 mM.

Fapyane et al. [117] reported the possibility to fabricate an urea amperometric biosensor by monitoring the CO_2 that is released from the urease in presence of the substrate. The system is based on a CO_2 microsensor equipped by a gas permeable membrane with a gap filled with a buffer solution containing urease and a sensing Ag wire dipped in an ionic liquid (Fig. 6d). An external silicon membrane is in contact with the sample solution. In this condition, urea can migrate in the urease-buffer solution; the produced CO_2 diffuse through the gas permeable membrane to the ionic liquid medium; in this water free
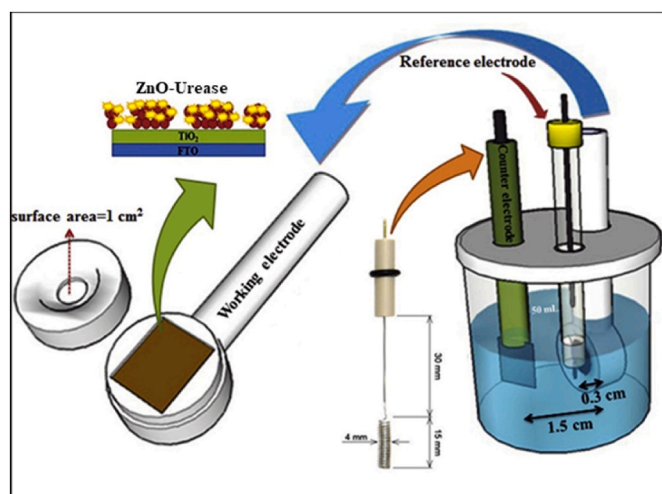
Fig. 7. Examples of EIS-urea biosensor: Schematic representation of the measurement setup and the Urease/Nano-ZnO/TiO2/Fluorinated-Tin Oxide (FTO) working electrode (Reproduced with permission from Ref. [120]).

environment, the Ag microsensor can reduce the CO_2 to $CO_2^{\bullet-}$. The reported urea biosensor has a linear range from 0 to 1000 μM with a LOD of 0.94 μM.

Another electroanalytical approach used for urea detection is based on Electrochemical Impedance Spectroscopy (EIS) [118]. A disposable copper tape-based electrode, covered with layers of wax, urease, and poly(methyl methacrylate) (PMMA) was developed by Bose et al. [119] for non-faradaic impedimetric sensing of urea. In this set-up, a wax layer keeps a paper–dielectric sensor dry, even in aqueous media. During the measurement, the sensor is dipped into the urea solution. The enzymatic hydrolysis of urea produces ammonium and carbonate ions, reducing the solution resistance and creating a measurable variation in impedance, useful to quantify total urea. A working range of 0.16–175 mM (corresponding to 1–1050 mg/dL) is reported [119]. An example of faradaic impedance measurements is described in Ref. [120] and shown in Fig. 7. The analytical signal is due to the redox reaction of NH_3 at the Urs/Nano-ZnO/TiO2/Fluorinated-Tin Oxide (FTO) electrode surface. The TiO2 substrate promotes electron transfer between ZnO to FTO electrode, by the formation of heterojunctions with ZnO.

Other examples of enzyme based amperometric assays are shown in Table 5.

Examples of non-enzymatic quantification of urea are also reported. Liu et al. [70], developed a flexible biosensor for the indirect quantification, monitoring the signal decrease of the redox species Fe^{II}/Fe^{III}, using a Molecular Imprinted Polymers (MIPs) sensing layer. In this approach, the electropolymerization of 3,4-ethylenedioxythiophene (EDOT) was used for the MIP layer development. The reported linearity range was between 1 and 100 mM and the LOD was 0.1 mM.

An alternative strategy for the determination of urea through an enzyme-free, indirect approach was proposed by Vasconcellos et al. [127] and it takes advantage from the presence of Cl^- ions in solution. In this case a suitable electrode material could be used to generate chlorine from the electrochemical oxidation of chloride following reaction (2) [54]. Evolved chlorine quickly dissociates in water yielding

Table 5
Some examples of indirect urease-based voltammetric/amperometric sensors with the reported analytical features and the type of real samples analyzed.

Materials	Measure	Linearity Range (M)	Detection Limit (M)	Real Sample	Response Time (sec)	Stability (days)	Reference
Urs -(MWCNTs)-Ferrocene-poly(amidoamine)- Pencil graphite electrode (PGE)	Amperometric	2×10^{-4} - 1.8×10^{-3}	5×10^{-5}	Blood	3	3	[112]
Urs-Nafion- MWCNT- PANI-Fe3O4-GCE	CV, DPV, CA	1.0×10^{-3} - 2.50×10^{-2}	6.7×10^{-5}	Milk	–	60	[113]
Urs-CuF-PANI-Nafion-GCE	DPV	5×10^{-7} - 4.5×10^{-5}	1.7×10^{-7}	Soil Milk	–	7	[114]
Urs-CoF-PANI-Nafion-GCE		5×10^{-7} - 4.5×10^{-5}	2.3×10^{-7}				
Urs-NIF-PANI-Nafion-GCE		5×10^{-7} - 4.5×10^{-5}	3.7×10^{-7}				
Urs-ZnF-PANI-Nafion-GCE		5×10^{-7} - 4.5×10^{-5}	4.2×10^{-7}				
Urs-Graphitized nanodiamond-Graphene nanoplatelet- Screen Printed Electrodes (SPEs)	Amperometric	1.6×10^{-3} - 15×10^{-3}	8×10^{-5}	Milk	20	15	[115]
Dyalisis membrane/Urs solution/Ionic Liquid/Ag	Amperometric	0 - 1000×10^{-6}	1×10^{-6}	Blood Plasma	120	<14	[117]
Urs-Nano ZnO-TiO2-FTO	Impedimetric	5×10^{-4} - 3.4×10^{-2}	3×10^{-4}	Serum	4	28	[120]
Urs-Polyaniline-Sulfonated Graphene- ITO	Amperometric	1.2×10^{-4} - 1.23×10^{-2}	50×10^{-5}	Urine	5	15	[121]
Urs-Clinoptilolite Zeolite modified Electrode	Conductimetric	0 - 64×10^{-3}	10^{-6}	Urine Blood	40 to 70	150	[122]
Urs-ZnO-MWCNT-ITO	CV	1.6×10^{-3} - 1.6×10^{-2}	2.3×10^{-4}	Serum	4	120	[123]
Urs-PVA conducting hydrogel membrane-PANI grafed polyacrylamide-GCE	DPV, EIS	1.5×10^{-6} - 1×10^{-3}	6×10^{-8}	Milk Urine Serum Soil Puffed Rice	10	60	[124]
Urs-ZnO-F-doped SnO2	Impedimetric	1.3×10^{-3} - 1.8×10^{-3}	8.3×10^{-4}	Serum	10	21	[125]
Urs-Nano ZnO-FTO	Impedimetric	8.3×10^{-4} - 2.324×10^{-2}	4.0×10^{-4}	Serum	4	42	[126]

Urs: Urease; ITO: Indium Tin Oxide; PANI: Polyaniline; MWCNT: Multi-Walled Carbon Nanotubes; GCE: Glassy Carbon Electrode; SF: Silk Fibroin; PVA: Polyvinyl Alcohol; FTO: Fluorinated-Tin Oxide; EIS: Electrochemical impedance spectroscopy; CV: Cyclic voltammetry; CA: Chronoamperometry; DPV: Differential pulse voltammetry.

hypochlorous acid according to reaction (3), in which speciation is defined by the acid-base equilibria of reaction (4).

$$2Cl^- \rightarrow Cl_2 + 2e^- \tag{2}$$

$$Cl_{2(aq)} + H_2O \rightarrow HClO + Cl^- + H^+ \tag{3}$$

$$HClO \rightleftharpoons ClO^- + H^+, pKa = 7.55 \tag{4}$$

Electrogenerated active chlorine species from reactions (2)–(4) react with urea yielding N_2 (5).

$$(NH_2)_2CO + 3ClO^- \rightarrow N_2 + CO_2 + 3Cl^- + H_2O \tag{5}$$
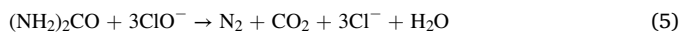
The chemical reaction that consumes electrogenerated active chlorine species can be used to quantify the concentration of urea in solutions [127]. This method can allow urea quantification with a LOD of 1.83×10^{-6} M and a linear range of 6.66×10^{-6} to 3.33×10^{-4} M.

4. Conclusions & further perspectives

In this work different methods for direct and indirect electrochemical determination of urea have been revised. Indirect electrochemical methodologies exhibit intriguing features for various applications, offering high selectivity due to the reliance on the enzymatic reagent but also leading to stability issues over time. By contrast, direct electrochemical methods show interesting features in terms of stability and cost-effectiveness but suffer in selectivity. AI-based methodologies have the potential to facilitate the creation of smart sensors capable of adapting to dynamic environments and delivering instantaneous feedback. Additionally, AI-based approaches can aid in optimizing sensor performance and offer a real-time feedback of the identified analyte. Recent advancements in AI and ML have proven useful in data processing for real sample analysis, enhancing biosensor development. AI and ML techniques analyze large datasets, identify patterns, and optimize experimental conditions for increased sensitivity and selectivity [128]. AI-based biosensors hold potential for simultaneous detection of multiple substances using electrodes with different analyte response characteristics. AI can also optimize parameters in industrial chemical processes, as demonstrated in a study on ceramic-based microbial fuel cells (CMFCs) [129] or in the monitoring and prediction of blood urea and glucose in Chronical Kidney Disease Patients [130], in environmental science with studies about the urea release as fertilizer [131].

By leveraging the capabilities of nanomaterials and AI-based approaches, could be possible to push the boundaries of sensor technology and renewable energy solutions, leading to more efficient, cost-effective, and environmentally friendly solutions for urea detection.

Author contributions

"All authors have read and agreed to the published version of the manuscript." LQ: Writing - original draft; SL: Writing - original draft, Supervision; FC: supervision; CC: supervision; IP: Writing - original draft, Supervision, Project administration.

Declaration of competing interest

The authors declare that they have no known competing financial interests or personal relationships that could have appeared to influence the work reported in this paper.

Data availability

No data was used for the research described in the article.

Acknowledgments

References

[1] J. Häberle, N. Boddaert, A. Burlina, A. Chakrapani, M. Dixon, M. Huemer, D. Karall, D. Martinelli, P. Crespo, R. Santer, A. Servais, V. Valayannopoulos, M. Lindner, V. Rubio, C. Dionisi-Vici, Suggested guidelines for the diagnosis and management of urea cycle disorders, Orphanet J. Rare Dis. 7 (2012) 32, https://doi.org/10.1186/1750-1172-7-32.

[2] S.N. Botewad, D.K. Gaikwad, N.B. Girhe, H.N. Thorat, P.P. Pawar, Urea biosensors: a comprehensive review, Biotechnol. Appl. Biochem. (2021), https://doi.org/10.1002/bab.2168.

[3] https://www.esamed.it/en/products/human-line/point-of-care-testing-en/automatic-dry-biochemical-analyzer-sd1/ (accessed on 30/05/2023), (n.d.).

[4] https://lifetest.dk/en/product/insight-minichem-analyser-si-units-urea-mmol-l-ua-umol-l-crea-umol-l/ (Accessed on 30/05/2023), (n.d.).

[5] https://it.lysunbio.com/ (Accessed on 30/05/2023), (n.d.).

[6] https://www.globalpointofcare.abbott/en/index.html (Accessed on 30/05/2023), (n.d.).

[7] R. Larcher, M. Lottelier, S. Badiou, A.-M. Dupuy, A.-S. Bargnoux, J.-P. Cristol, Analytical performances of the novel i-STAT alinity point-of-care analyzer, Diagnostics 13 (2023) 297, https://doi.org/10.3390/diagnostics13020297.

[8] https://www.siemens-healthineers.com/blood-gas/blood-gas-systems/epoc-blood-analysis-system (Accessed on 30/05/2023), (n.d.).

[9] https://www.edan.com/product/e/i15_Blood_Gas_and_Chemistry_Analysis_System.html (Accessed on 30/05/2023), (n.d.).

[10] https://www.radiometer.com/en/products/blood-gas-testing/abl90-flex-plus-blood-gas-analyzer (Accessed on 30/05/2023), (n.d.).

[11] A.-S. Bargnoux, N. Kuster, T. Sutra, L. Laroche, A. Rodriguez, M. Morena, L. Chenine, L. Chalabi, A.-M. Dupuy, S. Badiou, J.-P. Cristol, Evaluation of a new point-of-care testing for creatinine and urea measurement, Scand. J. Clin. Lab. Invest. 81 (2021) 290–297, https://doi.org/10.1080/00365513.2021.1914344.

[12] S.N. Botewad, D.K. Gaikwad, N.B. Girhe, H.N. Thorat, P.P. Pawar, Urea biosensors: a comprehensive review, Biotechnol. Appl. Biochem. 70 (2023) 485–501, https://doi.org/10.1002/bab.2168.

[13] C.S. Pundir, S. Jakhar, V. Narwal, Determination of urea with special emphasis on biosensors: a review, Biosens. Bioelectron. 123 (2019) 36–50, https://doi.org/10.1016/j.bios.2018.09.067.

[14] Z. Zhao, J. Xiao, X. Zhang, J. Jiang, M. Zhang, Y. Li, T. Li, J. Wang, A thread-based micro device for continuous electrochemical detection of saliva urea, Microchem. J. 190 (2023), 108634, https://doi.org/10.1016/j.microc.2023.108634.

[15] D.J. Saldanha, A. Cai, N.-M. Dorval Courchesne, The evolving role of proteins in wearable sweat biosensors, ACS Biomater. Sci. Eng. 9 (2023) 2020–2047, https://doi.org/10.1021/acsbiomaterials.1c00699.

[16] P. Schimmel, L. Kleinjans, R.S. Bongers, J. Knol, C. Belzer, Breast milk urea as a nitrogen source for urease positive Bifidobacterium infantis, FEMS Microbiol. Ecol. 97 (2021), https://doi.org/10.1093/femsec/fiab019.

[17] W.D. Gould, C. Hagedorn, R.G.L. McCready, in: Urea Transformations and Fertilizer Efficiency in Soil, 1986, pp. 209–238, https://doi.org/10.1016/S0065-2113(08)60283-7.

[18] B. Gagnon, N. Ziadi, C. Grant, Urea fertilizer forms affect grain corn yield and nitrogen use efficiency, Can. J. Soil Sci. 92 (2012) 341–351, https://doi.org/10.4141/cjss2011-074.

[19] V. Dhanushkodi, T.B. Priyadharshini, M. Baskar, S. Meena, K. Senthil, T. U. Maheshwari, Slow and controlled release nitrogen fertilizers: options for improving rice productivity: a review, Int J Plant Soil Sci (2022) 970–981, https://doi.org/10.9734/ijpss/2022/v34i242726.

[20] M. Pan, G. Heinecke, S. Bernardo, C. Tsui, J. Levitt, Urea: a comprehensive review of the clinical literature, Dermatol. Online J. 19 (2013), https://doi.org/10.5070/D31911020392.

[21] T.A. Currier, D.W. Bohnert, S.J. Falck, S.J. Bartle, Daily and alternate day supplementation of urea or biuret to ruminants consuming low-quality forage: I. Effects on cow performance and the efficiency of nitrogen use in wethers1,2, J. Anim. Sci. 82 (2004) 1508–1517, https://doi.org/10.2527/2004.8251508x.

[22] M. Xia, C. Mao, A. Gu, A.A. Tountas, C. Qiu, T.E. Wood, Y.F. Li, U. Ulmer, Y. Xu, C.J. Viasus, J. Ye, C. Qian, G. Ozin, Solar urea: towards a sustainable fertilizer industry, Angew. Chem. 134 (2022), https://doi.org/10.1002/ange.202110158.

[23] D. Weerakoon, B. Bansal, L.P. Padhye, A. Rachmani, L. James Wright, G. Silyn Roberts, S. Baroutian, A critical review on current urea removal technologies from water: an approach for pollution prevention and resource recovery, Sep. Purif. Technol. 314 (2023), 123652, https://doi.org/10.1016/j.seppur.2023.123652.

[24] P.M. Glibert, J. Harrison, C. Heil, S. Seitzinger, Escalating worldwide use of urea – a global change contributing to coastal eutrophication, Biogeochemistry 77 (2006) 441–463, https://doi.org/10.1007/s10533-005-3070-5.

[25] P.M. Glibert, T.M. Trice, B. Michael, L. Lane, Urea in the tributaries of the chesapeake and coastal bays of Maryland, Water Air Soil Pollut. 160 (2005) 229–243, https://doi.org/10.1007/s11270-005-2546-1.

[26] M. Latkar, T. Chakrabarti, Performance of upflow anaerobic sludge blanket reactor carrying out biological hydrolysis of urea, Water Environ. Res. 66 (1994) 12–15, https://doi.org/10.2175/WER.66.1.3.

[27] Y. Chen, H. Chen, Z. Chen, H. Hu, C. Deng, X. Wang, The benefits of autotrophic nitrogen removal from high concentration of urea wastewater through a process of urea hydrolysis and partial nitritation in sequencing batch reactor, J. Environ. Manag. 292 (2021), 112762, https://doi.org/10.1016/j.jenvman.2021.112762.

[28] P.S. Francis, S.W. Lewis, K.F. Lim, Analytical methodology for the determination of urea: current practice and future trends, TrAC, Trends Anal. Chem. 21 (2002) 389–400, https://doi.org/10.1016/S0165-9936(02)00507-1.

[29] W.T. Bolleter, C.J. Bushman, P.W. Tidwell, Spectrophotometric determination of ammonia as indophenol, Anal. Chem. 33 (1961) 592–594, https://doi.org/10.1021/ac60172a034.

[30] O. Özbek, C. Berkel, Ö. Isildak, I. Isildak, Potentiometric urea biosensors, Clin. Chim. Acta 524 (2022) 154–163, https://doi.org/10.1016/j.cca.2021.11.011.

[31] M.K. Reay, C.A. Yates, P.J. Johnes, C.J. Arthur, D.L. Jones, R.P. Evershed, High resolution HPLC-MS confirms overestimation of urea in soil by the diacetyl monoxime (DAM) colorimetric method, Soil Biol. Biochem. 135 (2019) 127–133, https://doi.org/10.1016/j.soilbio.2019.04.015.

[32] J. Zhou, C. Liu, Y. Chen, X. Luo, D. Deng, Determination of urea in swimming pool water using high-performance liquid chromatography with online postcolumn derivatization by xanthydrol, J. Chromatogr. Sci. 61 (2023) 339–346, https://doi.org/10.1093/chromsci/bmac025.

[33] E. Reynoso, E. Torres, F. Bettazzi, I. Palchetti, Trends and perspectives in immunosensors for determination of currently-used pesticides: the case of glyphosate, organophosphates, and neonicotinoids, Biosensors 9 (2019) 20, https://doi.org/10.3390/bios9010020.

[34] P.S. Sfragano, G. Moro, F. Polo, I. Palchetti, The role of peptides in the design of electrochemical biosensors for clinical diagnostics, Biosensors 11 (2021) 246, https://doi.org/10.3390/bios11080246.

[35] I. Palchetti, C. Upjohn, A.P.F. Turner, M. Mascini, Disposable screen-printed electrodes (spe) mercury-free for lead detection, Anal. Lett. 33 (2000) 1231–1246, https://doi.org/10.1080/00032710008543119.

[36] G.G. Guilbault, J.G. Montalvo, Urea-specific enzyme electrode, J. Am. Chem. Soc. 91 (1969) 2164–2165, https://doi.org/10.1021/ja01036a083.

[37] G.G. Guilbault, E. Hrabankova, Electrode for determination of amino acids, Anal. Chem. 42 (1970) 1779–1783, https://doi.org/10.1021/ac50160a052.

[38] G.G. Guilbault, J.G. Montalvo, Enzyme electrode for the substrate urea, J. Am. Chem. Soc. 92 (1970) 2533–2538, https://doi.org/10.1021/ja00711a052.

[39] P.H. Weiner, J.F. Parcher, Improved urea electrode, Anal. Chem. 45 (1973) 417–419, https://doi.org/10.1021/ac60324a053.

[40] G.G. Guilbault, F.R. Shu, Enzyme electrodes based on the use of a carbon dioxide sensor. Urea and L-tyrosine electrodes, Anal. Chem. 44 (1972) 2161–2166, https://doi.org/10.1021/ac60321a023.

[41] M. Mascini, G.G. Guilbault, Urease coupled ammonia electrode for urea determination in blood serum, Anal. Chem. 49 (1977) 795–798, https://doi.org/10.1021/ac50014a031.

[42] C. Eggenstein, M. Borchardt, C. Diekmann, Bernd Gründig, C. Dumschat, K. Cammann, M. Knoll, Friedrich Spener, A disposable biosensor for urea determination in blood based on an ammonium-sensitive transducer, Biosens. Bioelectron. 14 (1999) 33–41, https://doi.org/10.1016/S0956-5663(98)00103-1.

[43] F. Silva, Potentiometric determination of urea by sequential injection using Jack bean meal crude extract as a source of urease, Talanta 53 (2000) 331–336, https://doi.org/10.1016/S0039-9140(00)00490-2.

[44] T. Anfält, A. Graneli, D. Jagner, A urea electrode based on the ammonia probe, Anal. Lett. 6 (1973) 969–975, https://doi.org/10.1080/00032717308058175.

[45] A. Senillou, N. Jaffrezic-Renault, C. Martelet, S. Cosnier, A miniaturized urea sensor based on the integration of both ammonium based urea enzyme field effect transistor and a reference field effect transistor in a single chip, Talanta 50 (1999) 219–226, https://doi.org/10.1016/S0039-9140(99)00122-8.

[46] M. SINGH, N. Verma, A. Garg, N. Redhu, Urea biosensors, Sensor. Actuator. B Chem. 134 (2008) 345–351, https://doi.org/10.1016/j.snb.2008.04.025.

[47] D.A. Daramola, D. Singh, G.G. Botte, Dissociation rates of urea in the presence of NiOOH catalyst: a DFT analysis, J. Phys. Chem. A 114 (2010) 11513–11521, https://doi.org/10.1021/jp105159t.

[48] F. Guo, K. Ye, M. Du, X. Huang, K. Cheng, G. Wang, D. Cao, Electrochemical impedance analysis of urea electro-oxidation mechanism on nickel catalyst in alkaline medium, Electrochim. Acta 210 (2016) 474–482, https://doi.org/10.1016/j.electacta.2016.05.149.

[49] V. Vedharathinam, G.G. Botte, Experimental investigation of potential oscillations during the electrocatalytic oxidation of urea on Ni catalyst in alkaline medium, J. Phys. Chem. C 118 (2014) 21806–21812, https://doi.org/10.1021/jp5052529.

[50] V. Vedharathinam, G.G. Botte, Direct evidence of the mechanism for the electro-oxidation of urea on Ni(OH)2 catalyst in alkaline medium, Electrochim. Acta 108 (2013) 660–665, https://doi.org/10.1016/j.electacta.2013.06.137.

[51] S. Singh, M. Sharma, G. Singh, Recent advancements in urea biosensors for biomedical applications, IET Nanobiotechnol. 15 (2021) 358–379, https://doi.org/10.1049/nbt2.12050.

[52] H.D. Mai, G.Y. Sung, H. Yoo, Fabrication of nickel oxide nanostructures with high surface area and application for urease-based biosensor for urea detection, RSC Adv. 5 (2015) 78807–78814, https://doi.org/10.1039/C5RA14103F.

[53] D. Zhu, H. Zhang, J. Miao, F. Hu, L. Wang, Y. Tang, M. Qiao, C. Guo, Strategies for designing more efficient electrocatalysts towards the urea oxidation reaction, J Mater Chem A Mater 10 (2022) 3296–3313, https://doi.org/10.1039/D1TA09989B.

[54] X. Wang, J. Li, Y. Duan, J. Li, H. Wang, X. Yang, M. Gong, Electrochemical urea oxidation in different environment: from mechanism to devices, ChemCatChem 14 (2022), https://doi.org/10.1002/cctc.202101906.

[55] K.J. Babu, N. Senthilkumar, A.R. Kim, G.G. kumar, Freestanding and binder free PVDF-HFP/Ni-Co nanofiber membrane as a versatile platform for the electrocatalytic oxidation and non-enzymatic detection of urea, Sensor. Actuator. B Chem. 241 (2017) 541–551, https://doi.org/10.1016/j.snb.2016.10.069.

[56] S. Amin, A. Tahira, A. Solangi, V. Beni, J.R. Morante, X. Liu, M. Falhman, R. Mazzaro, Z.H. Ibupoto, A. Vomiero, A practical non-enzymatic urea sensor based on NiCo 2 O 4 nanoneedles, RSC Adv. 9 (2019) 14443–14451, https://doi.org/10.1039/C9RA00909D.

[57] C. Bao, Q. Niu, Z.-A. Chen, X. Cao, H. Wang, W. Lu, Ultrathin nickel-metal–organic framework nanobelt based electrochemical sensor for the determination of urea in human body fluids, RSC Adv. 9 (2019) 29474–29481, https://doi.org/10.1039/C9RA05716A.

[58] J. Yoon, Y.S. Yoon, D.-J. Kim, Silver-nanoparticle-decorated NiOOH nanorods for electrocatalytic urea sensing, ACS Appl. Nano Mater. 3 (2020) 7651–7658, https://doi.org/10.1021/acsanm.0c01279.

[59] Y.-T. Chen, P.-Y. Chen, S.-P. Ju, Preparation of Ni nanotube-modified electrodes via galvanic displacement on sacrificial Zn templates: solvent effects and attempts for non-enzymatic electrochemical detection of urea, Microchem. J. 158 (2020), 105172, https://doi.org/10.1016/j.microc.2020.105172.

[60] T.S. Sunil Kumar Naik, S. Saravanan, K.N. Sri Saravana, U. Pratiush, P.C. Ramamurthy, A non-enzymatic urea sensor based on the nickel sulfide/graphene oxide modified glassy carbon electrode, Mater. Chem. Phys. 245 (2020), 122798, https://doi.org/10.1016/j.matchemphys.2020.122798.

[61] T.Q.N. Tran, S.W. Yoon, B.J. Park, H.H. Yoon, CeO2-modified LaNi0.6Fe0.4O3 perovskite and MWCNT nanocomposite for electrocatalytic oxidation and detection of urea, J. Electroanal. Chem. 818 (2018) 76–83, https://doi.org/10.1016/j.jelechem.2018.04.003.

[62] T.Q.N. Tran, G. Das, H.H. Yoon, Nickel-metal organic framework/MWCNT composite electrode for non-enzymatic urea detection, Sensor. Actuator. B Chem. 243 (2017) 78–83, https://doi.org/10.1016/j.snb.2016.11.126.

[63] R. Sha, K. Komori, S. Badhulika, Graphene–Polyaniline composite based ultra-sensitive electrochemical sensor for non-enzymatic detection of urea, Electrochim. Acta 233 (2017) 44–51, https://doi.org/10.1016/j.electacta.2017.03.043.

[64] J. Yoon, M. Sim, T.-S. Oh, Y.S. Yoon, D.-J. Kim, Flexible electrochemical sensor based on NiCu(OOH) for monitoring urea in human sweat, J. Electrochem. Soc. 168 (2021), 117510, https://doi.org/10.1149/1945-7111/ac34ca.

[65] F. Cui, Y. Yue, Y. Zhang, Z. Zhang, H.S. Zhou, Advancing biosensors with machine learning, ACS Sens. 5 (2020) 3346–3364, https://doi.org/10.1021/acssensors.0c01424.

[66] H. Chen, E. Kätelhön, R.G. Compton, Machine learning in fundamental electrochemistry: recent advances and future opportunities, Curr. Opin. Electrochem. 38 (2023), 101214, https://doi.org/10.1016/j.coelec.2023.101214.

[67] B. Zambelli, F. Musiani, S. Benini, S. Ciurli, Chemistry of Ni 2+ in urease: sensing, trafficking, and catalysis, Acc. Chem. Res. 44 (2011) 520–530, https://doi.org/10.1021/ar200041k.

[68] M.S. Ghauri, J.D.R. Thomas, Evaluation of an ammonium ionophore for use in poly(vinyl chloride) membrane ion-selective electrodes: solvent mediator effects, Analyst 119 (1994) 2323, https://doi.org/10.1039/an9941902323.

[69] P. Kumar, P. Ramulu Lambadi, N. Kumar Navani, Non-enzymatic detection of urea using unmodified gold nanoparticles based aptasensor, Biosens. Bioelectron. 72 (2015) 340–347, https://doi.org/10.1016/j.bios.2015.05.029.

[70] Y.L. Liu, R. Liu, Y. Qin, Q.F. Qiu, Z. Chen, S.B. Cheng, W.H. Huang, Flexible electrochemical urea sensor based on surface molecularly imprinted nanotubes for detection of human sweat, Anal. Chem. 90 (2018) 13081–13087, https://doi.org/10.1021/acs.analchem.8b04223.

[71] G. Palleschi, M. Mascini, E. Martinez-fabregas, S. Alegret, Urea determination in human sera with an ammonium ion selective electrode made with solid inner electric contact and immobilised urease, Anal. Lett. 21 (1988) 1115–1129, https://doi.org/10.1080/00032718808055500.

[72] I. Wałcerz, R. Koncki, E. Leszczyńska, B. Salamonowicz, S. Głąb, Urea biosensors based on PVC membrane ion-selective electrodes, Anal. Lett. 29 (1996) 1939–1953, https://doi.org/10.1080/00032719608000800.

[73] Y. Kan, An all-solid-state ammonium ion-selective electrode based on polyaniline as transducer and poly (o-phenylenediamine) as sensitive membrane, Int. J. Electrochem. Sci. (2016) 9928–9940, https://doi.org/10.20964/2016.12.03.

[74] J. Hu, A. Stein, P. Bühlmann, Rational design of all-solid-state ion-selective electrodes and reference electrodes, TrAC, Trends Anal. Chem. 76 (2016) 102–114, https://doi.org/10.1016/j.trac.2015.11.004.

[75] M.E. Meyerhoff, Polymer membrane electrode based potentiometric ammonia gas sensor, Anal. Chem. 52 (1980) 1532–1534, https://doi.org/10.1021/ac50059a037.

[76] K.A. Erickson, P. Wilding, Evaluation of a novel point-of-care system, the i-STAT portable clinical analyzer, Clin. Chem. 39 (1993) 283–287, https://doi.org/10.1093/clinchem/39.2.283.

[77] P.S. Sfragano, S. Laschi, I. Palchetti, Sustainable printed electrochemical platforms for greener analytics, Front. Chem. 8 (2020), https://doi.org/10.3389/fchem.2020.00644.

[78] S. Laschi, Palchetti Ilaria, G. Marrazza, M. Mascini, Development of Disposable Low Density Screen-Printed Electrode Arrays for Simultaneous Electrochemical Measurements of the Hybridisation Reaction, Journal of Electroanalytical Chemistry 593 (2006) 211–218. https://doi.org/10.1016/j.jelechem.2006.04.015.

[79] C.S. Kushwaha, P. Singh, N.S. Abbas, S.K. Shukla, Self-activating zinc oxide encapsulated polyaniline-grafted chitosan composite for potentiometric urea sensor, J. Mater. Sci. Mater. Electron. 31 (2020) 11887–11896, https://doi.org/10.1007/s10854-020-03743-7.

[80] S. Jakhar, C.S. Pundir, Preparation, characterization and application of urease nanoparticles for construction of an improved potentiometric urea biosensor, Biosens. Bioelectron. 100 (2018) 242–250, https://doi.org/10.1016/j.bios.2017.09.005.

[81] Y.-H. Nien, T.-Y. Su, C.-S. Ho, J.-C. Chou, C.-H. Lai, P.-Y. Kuo, Z.-X. Kang, Z.-X. Dong, T.-Y. Lai, C.-H. Wang, The analysis of potentiometric flexible arrayed urea biosensor modified by graphene oxide and γ-Fe $_2$ O $_3$ nanoparticles, IEEE Trans. Electron. Dev. 67 (2020) 5104–5110, https://doi.org/10.1109/TED.2020.3023067.

[82] B. Öndeş, F. Akpınar, M. Uygun, M. Muti, D. Aktaş Uygun, High stability potentiometric urea biosensor based on enzyme attached nanoparticles, Microchem. J. 160 (2021) 105667, https://doi.org/10.1016/j.microc.2020.105667.

[83] H.J.N.P.D. Mello, M. Mulato, Enzymatically functionalized polyaniline thin films produced with one-step electrochemical immobilization and its application in glucose and urea potentiometric biosensors, Biomed. Microdevices 22 (2020), https://doi.org/10.1007/s10544-020-00478-4.

[84] F. Kuralay, H. Özyörük, A. Yıldız, Potentiometric enzyme electrode for urea determination using immobilized urease in poly(vinylferrocenium) film, Sensor. Actuator. B Chem. 109 (2005) 194–199, https://doi.org/10.1016/j.snb.2004.12.043.

[85] M. Gutiérrez, S. Alegret, M. del Valle, Potentiometric bioelectronic tongue for the analysis of urea and alkaline ions in clinical samples, Biosens. Bioelectron. 22 (2007) 2171–2178, https://doi.org/10.1016/j.bios.2006.10.007.

[86] D. Chirizzi, C. Malitesta, Potentiometric urea biosensor based on urease immobilized by an electrosynthesized poly(o-phenylenediamine) film with buffering capability, Sensor. Actuator. B Chem. 157 (2011) 211–215, https://doi.org/10.1016/j.snb.2011.03.051.

[87] S.M.U. Ali, Z.H. Ibupoto, S. Salman, O. Nur, M. Willander, B. Danielsson, Selective determination of urea using urease immobilized on ZnO nanowires, Sensor. Actuator. B Chem. 160 (2011) 637–643, https://doi.org/10.1016/j.snb.2011.08.041.

[88] S.V. Marchenko, I.S. Kucherenko, A.N. Hereshko, I.V. Panasiuk, O.O. Soldatkin, A.V. El'skaya, A.P. Soldatkin, Application of potentiometric biosensor based on recombinant urease for urea determination in blood serum and hemodialyzate, Sensor. Actuator. B Chem. 207 (2015) 981–986, https://doi.org/10.1016/j.snb.2014.06.136.

[89] B. Liu, R. Hu, J. Deng, Studies on a potentiometric urea biosensor based on an ammonia electrode and urease, immobilized on γ-aluminum oxide matrix, Anal. Chim. Acta 341 (1997) 161–169, https://doi.org/10.1016/S0003-2670(96)00553-3.

[90] S.K. Jha, A. Topkar, S.F. D'Souza, Development of potentiometric urea biosensor based on urease immobilized in PVA–PAA composite matrix for estimation of blood urea nitrogen (BUN), J. Biochem. Biophys. Methods 70 (2008) 1145–1150, https://doi.org/10.1016/j.jprot.2007.12.006.

[91] X. Chen, Z. Yang, S. Si, Potentiometric urea biosensor based on immobilization of urease onto molecularly imprinted TiO2 film, J. Electroanal. Chem. 635 (2009) 1–6, https://doi.org/10.1016/j.jelechem.2009.07.005.

[92] T. Ahuja, D. Kumar, N. Singh, A.M. Biradar, Rajesh, Potentiometric urea biosensor based on multi-walled carbon nanotubes (MWCNTs)/silica composite material, Mater. Sci. Eng. C 31 (2011) 90–94, https://doi.org/10.1016/j.msec.2010.08.001.

[93] K. Saeedfar, L. Heng, T. Ling, M. Rezayi, Potentiometric urea biosensor based on an immobilised fullerene-urease bio-conjugate, Sensors 13 (2013) 16851–16866, https://doi.org/10.3390/s131216851.

[94] R.O. Flores, L. Maria, C. Silva, A.F. Melo, A.M. Salgado, Analysis of potential applicability of the potentiometric urea biosensor to real samples. www.aidic.it/cet, 2013.

[95] W. Prissanaroon-Ouajai, A. Sirivat, P.J. Pigram, N. Brack, Potentiometric urea biosensor based on a urease-immobilized polypyrrole, Macromol. Symp. 354 (2015) 334–339, https://doi.org/10.1002/masy.201400087.

[96] R. Ramesh, P. Puhazhendi, J. Kumar, M.K. Gowthaman, S.F. D'Souza, N.R. Kamini, Potentiometric biosensor for determination of urea in milk using immobilized Arthrobacter creatinolyticus urease, Mater. Sci. Eng. C 49 (2015) 786–792, https://doi.org/10.1016/j.msec.2015.01.048.

[97] A.N. Reshetilov, Y.V. Plekhanova, S.A. Tikhonenko, A.V. Dubrovskii, Polyelectrolyte microcapsules with urease and paramagnetic particles as a basis for a potentiometric biosensor for determining urea, J. Anal. Chem. 70 (2015) 1368–1372, https://doi.org/10.1134/S1061934815110032.

[98] J. Magalhães, Urea potentiometric biosensor based on urease immobilized on chitosan membranes, Talanta 47 (1998) 183–191, https://doi.org/10.1016/S0039-9140(98)00066-6.

[99] M.-J. Syu, Y.-S. Chang, Ionic effect investigation of a potentiometric sensor for urea and surface morphology observation of entrapped urease/polypyrrole matrix, Biosens. Bioelectron. 24 (2009) 2671–2677, https://doi.org/10.1016/j.bios.2009.01.036.

[100] P. Pandey, Tetraphenylborate doped polyaniline based novel pH sensor and solid-state urea biosensor, Talanta 55 (2001) 773–782, https://doi.org/10.1016/S0039-9140(01)00505-7.

[101] S. Komaba, M. Seyama, T. Momma, T. Osaka, Potentiometric biosensor for urea based on electropolymerized electroinactive polypyrrole, Electrochim. Acta 42 (1997) 383–388, https://doi.org/10.1016/S0013-4686(96)00226-5.

[102] V. Bisht Rajesh, W. Takashima, K. Kaneto, Development of a potentiometric urea biosensor based on copolymer poly(N-3-aminopropyl pyrrole-co-pyrrole) film, React. Funct. Polym. 62 (2005) 51–59, https://doi.org/10.1016/j.reactfunctpolym.2004.08.009.

[103] T. Ahuja, I. Mir, D. Kumar, Rajesh, Potentiometric urea biosensor based on BSA embedded surface modified polypyrrole film, Sensor. Actuator. B Chem. 134 (2008) 140–145, https://doi.org/10.1016/j.snb.2008.04.020.

[104] U.B. Trivedi, D. Lakshminarayana, I.L. Kothari, N.G. Patel, H.N. Kapse, K.K. Makhija, P.B. Patel, C.J. Panchal, Potentiometric biosensor for urea determination in milk, Sensor. Actuator. B Chem. 140 (2009) 260–266, https://doi.org/10.1016/j.snb.2009.04.022.

[105] B. Lakard, D. Magnin, O. Deschaume, G. Vanlancker, K. Glinel, S. Demoustier-Champagne, B. Nysten, A.M. Jonas, P. Bertrand, S. Yunus, Urea potentiometric enzymatic biosensor based on charged biopolymers and electrodeposited polyaniline, Biosens. Bioelectron. 26 (2011) 4139–4145, https://doi.org/10.1016/j.bios.2011.04.009.

[106] L.T.M. Nguyen, H.H. Yoon, Potentiometric urea biosensor based on carbon nanotubes and polyion complex film, J. Nanosci. Nanotechnol. 15 (2015) 1150–1153, https://doi.org/10.1166/jnn.2015.9327.

[107] X. Mei, J. Yang, J. Liu, Y. Li, Wearable, nanofiber-based microfluidic systems with integrated electrochemical and colorimetric sensing arrays for multiplex sweat analysis, Chem. Eng. J. 454 (2023), 140248, https://doi.org/10.1016/j.cej.2022.140248.

[108] G. Ibáñez-Redín, G. Rosso Cagnani, N.O. Gomes, P.A. Raymundo-Pereira, S.A.S. Machado, M.A. Gutierrez, J.E. Krieger, O.N. Oliveira, Wearable potentiometric biosensor for analysis of urea in sweat, Biosens. Bioelectron. 223 (2023), 114994, https://doi.org/10.1016/j.bios.2022.114994.

[109] J. Ping, J. Wu, Y. Wang, Y. Ying, Simultaneous determination of ascorbic acid, dopamine and uric acid using high-performance screen-printed graphene electrode, Biosens. Bioelectron. 34 (2012) 70–76, https://doi.org/10.1016/j.bios.2012.01.016.

[110] F. Bettazzi, C. Ingrosso, P.S. Sfragano, V. Pifferi, L Falciola, ML Curri, I. Palchetti, Gold nanoparticles modified graphene platforms for highly sensitive electrochemical detection of vitamin C in infant food and formulae, Food Chemistry 344 (2021) 128692, https://doi.org/10.1016/j.foodchem.2020.128692.

[111] J. Ping, Y. Wang, J. Wu, Y. Ying, F. Ji, Determination of ascorbic acid levels in food samples by using an ionic liquid–carbon nanotube composite electrode, Food Chem. 135 (2012) 362–367, https://doi.org/10.1016/j.foodchem.2012.05.013.

[112] E. Dervisevic, M. Dervisevic, J.N. Nyangwebah, M. Şenel, Development of novel amperometric urea biosensor based on Fc-PAMAM and MWCNT bio-nanocomposite film, Sensor. Actuator. B Chem. 246 (2017) 920–926, https://doi.org/10.1016/j.snb.2017.02.122.

[113] A.K. Singh, M. Singh, N. Verma, Electrochemical preparation of Fe3O4/MWCNT-polyaniline nanocomposite film for development of urea biosensor and its application in milk sample, J. Food Meas. Char. 14 (2020) 163–175, https://doi.org/10.1007/s11694-019-00278-2.

[114] V. Sanko, A. Şenocak, S.O. Tümay, E. Demirbas, A novel comparative study for electrochemical urea biosensor design: effect of different ferrite nanoparticles (MFe2O4, M: Cu, Co, Ni, Zn) in urease immobilized composite system, Bioelectrochemistry 149 (2023), 108324, https://doi.org/10.1016/j.bioelechem.2022.108324.

[115] V. Kumar, I. Kaur, S. Arora, R. Mehla, K. Vellingiri, K.-H. Kim, Graphene nanoplatelet/graphitized nanodiamond-based nanocomposite for mediator-free electrochemical sensing of urea, Food Chem. 303 (2020), 125375, https://doi.org/10.1016/j.foodchem.2019.125375.

[116] K. Kim, J. Lee, B.M. Moon, Y.B. Seo, C.H. Park, M. Park, G.Y. Sung, Fabrication of a urea biosensor for real-time dynamic fluid measurement, Sensors (2018) 18, https://doi.org/10.3390/s18082607.

[117] D. Fapyane, D. Berillo, J.L. Marty, N.P. Revsbech, Urea biosensor based on a CO2 microsensor, ACS Omega 5 (2020) 27582–27590, https://doi.org/10.1021/acsomega.0c04146.

[118] H.S. Magar, R.Y.A. Hassan, A. Mulchandani, Electrochemical impedance spectroscopy (EIS): principles, construction, and biosensing applications, Sensors 21 (2021) 6578, https://doi.org/10.3390/s21196578.

[119] A. Bose, K. Biswas, Impedimetry-based disposable sensor for the detection of urea in aqueous media, IEEE Sensor. J. 23 (2023) 4185–4192, https://doi.org/10.1109/JSEN.2022.3232377.

[120] R. Rahmanian, S.A. Mozaffari, H.S. Amoli, M. Abedi, Development of sensitive impedimetric urea biosensor using DC sputtered Nano-ZnO on TiO2 thin film as a novel hierarchical nanostructure transducer, Sensor. Actuator. B Chem. 256 (2018) 760–774, https://doi.org/10.1016/j.snb.2017.10.009.

[121] S.S. An, H.H. Yoon, G. Das, Amperometric urea biosensors based on sulfonated graphene/polyaniline nanocomposite, Int. J. Nanomed. (2015) 55, https://doi.org/10.2147/IJN.S88315.

[122] O.Y. Saiapina, V.M. Pyeshkova, O.O. Soldatkin, V.G. Melnik, B.A. Kurç, A. Walcarius, S.V. Dzyadevych, N. Jaffrezic-Renault, Conductometric enzyme biosensors based on natural zeolite clinoptilolite for urea determination, Mater. Sci. Eng. C 31 (2011) 1490–1497, https://doi.org/10.1016/j.msec.2011.06.003.

[123] M. Tak, V. Gupta, M. Tomar, Zinc oxide–multiwalled carbon nanotubes hybrid nanocomposite based urea biosensor, J. Mater. Chem. B 1 (2013) 6392, https://doi.org/10.1039/c3tb20935k.

[124] J. Das, P. Sarkar, Enzymatic electrochemical biosensor for urea with a polyaniline grafted conducting hydrogel composite modified electrode, RSC Adv. 6 (2016) 92520–92533, https://doi.org/10.1039/C6RA12159D.

[125] R. Rahmanian, S.A. Mozaffari, M. Abedi, Disposable urea biosensor based on nanoporous ZnO film fabricated from omissible polymeric substrate, Mater. Sci. Eng. C 57 (2015) 387–396, https://doi.org/10.1016/j.msec.2015.08.004.

[126] S.A. Mozaffari, R. Rahmanian, M. Abedi, H.S. Amoli, Urea impedimetric biosensor based on reactive RF magnetron sputtered zinc oxide nanoporous transducer, Electrochim. Acta 146 (2014) 538–547, https://doi.org/10.1016/j.electacta.2014.08.105.

[127] M. de, L.S. Vasconcellos, L.R.G. Silva, C.S. Lee, A.S. Fajardo, S. Garcia-Segura, J. Ribeiro, Dimensionally stable anode based sensor for urea determination via linear sweep voltammetry, Sensors 21 (2021), https://doi.org/10.3390/s21103450.

[128] Z. Zhou, L. Wang, J. Wang, C. Liu, T. Xu, X. Zhang, Machine learning with neural networks to enhance selectivity of nonenzymatic electrochemical biosensors in multianalyte mixtures, ACS Appl. Mater. Interfaces 14 (2022) 52684–52690, https://doi.org/10.1021/acsami.2c17593.

[129] H. Rezk, A.G. Olabi, M.A. Abdelkareem, E.T. Sayed, Artificial intelligence as a novel tool for enhancing the performance of urine fed microbial fuel cell as an emerging approach for simultaneous power generation and wastewater treatment, J. Taiwan Inst. Chem. Eng. (2023), 104726, https://doi.org/10.1016/j.jtice.2023.104726.

[130] J. Parab, M. Sequeira, M. Lanjewar, C. Pinto, G. Naik, Backpropagation neural network-based machine learning model for prediction of blood urea and glucose in CKD Patients, IEEE J Transl Eng Health Med 9 (2021) 1–8, https://doi.org/10.1109/JTEHM.2021.3079714.

[131] Z. Jiang, S. Yang, X. Chen, Q. Pang, Y. Xu, S. Qi, W. Yu, H. Dai, Controlled release urea improves rice production and reduces environmental pollution: a research based on meta-analysis and machine learning, Environ. Sci. Pollut. Control Ser. 29 (2022) 3587–3599, https://doi.org/10.1007/s11356-021-15956-2.